© Indian Academy of Sciences

Experimental study and analysis of a thermoacoustically driven thermoacoustic refrigerator

A B DESAI[1,*] , K P DESAI[1], H B NAIK[1] and M D ATREY[2]

[1]Department of Mechanical Engineering, Sardar Vallbhbhai National Institute of Technology, Surat 395007, India
[2]Department of Mechanical Engineering, Indian Institute of Technology Bombay, Mumbai 400076, India
e-mail: abhinavbdesai@gmail.com

Abstract. Experimental investigations are performed on a half-wavelength standing wave type thermoacoustically driven thermoacoustic refrigerator also known as TADTAR. Present TADTAR device conceived to be a quarter wavelength standing wave type thermoacoustic engine (TAE) coupled to a quarter wavelength standing wave thermoacoustic refrigerator (TAR). A TAE generates acoustic work using heat, and this produced acoustic work is directly fed to TAR where a useful cooling effect is developed. The study here aims to project the enhancement in the performance of a TADTAR system by using better geometric choices and operating conditions. In the present work, by keeping the engine part unaltered, parametric variations on the refrigerator side are performed. Two geometric parameters namely resonator length and TAR stack position and one operating parameter, working gas, have been varied at three distinct choices. The performance of TADTAR is examined for three output parameters of TADTAR namely frequency of oscillations, pressure amplitude, and temperature difference across TAR stack. The present study should be useful for assisting select these parameters for starting the designing of a TADTAR. It also helps in concluding in a more generalized way the dependence of the above-said output of TADTAR on the varying parameters. This paper shows that longer resonator and He-Ar mixture as working gas among the choices is better for a TADTAR system for achieving better performance. It also highlights the potential existence of a unique position for a stack length for a TADTAR to attain maximum performance in terms of the temperature difference across the TAR stack. The present paper reports the maximum temperature difference of 16.3 K across the TAR stack.

Keywords. Thermoacoustic refrigeration; standing wave; TADTAR; mixture working gas; stack position; resonator length.

1. Introduction

Thermoacoustics, as the name suggests, involves the study of heat and acoustic interactions. In thermoacoustics, heat may be supplied to produce acoustic work, or acoustic work may be absorbed to realize the useful cooling effect. There are mainly two types of devices working on the principle of thermoacoustics. One is a thermoacoustic engine (TAE) which uses the heat to produce acoustic work and the other is a thermoacoustic refrigerator (TAR) which absorbs acoustic work to produce cooling effect across refrigerator stack. Usually, these thermoacoustic devices are of quarter wavelength type or half-wavelength type depending upon their physical construction.

Thermoacoustic heat pumping is relatively new technology but the reverse of this process i.e., sound generated because of temperature gradient had been observed for

several centuries by glassblowers. Rott [1–3] worked out the first mathematical model wherein he explained acoustic oscillations. He considered these oscillations being in a gaseous channel having an axial temperature gradient. However, Lord Rayleigh [4] provided the first thorough approximation of thermoacoustic oscillations. Interpreting the commencement of acoustic oscillations in fluid because of heat transfer, Rayleigh asserted that if heat is supplied to a gas at the instant of highest compression and removed at the most rarefied state, the oscillations are encouraged or intensified resulting in origination of acoustic power. Whereas acoustic power gets absorbed when the heat is removed from the gas at the moment of the greatest compression and provided to it at the time of the greatest rarefaction because of the dissipation of an acoustic wave.

Swift [5] provided a detailed discussion on the working of a thermoacoustic engine, and Tijani *et al* [6] provided the qualitative engineering approach to design a thermoacoustic refrigerator. The present work shows a combination system

---

*For correspondence

wherein a quarter wavelength standing wave type thermoacoustic engine is coupled directly with a quarter wavelength standing wave type thermoacoustic refrigerator to form an integrated half-wavelength standing wave type thermoacoustically driven thermoacoustic refrigerator (TADTAR). Figure 1 shows the schematic of a TADTAR, highlighting the key components and defining the stack position–the distance of the stack center from the closed end.

In the TAE section of a TADTAR, a steep temperature gradient is maintained across the stack to generate acoustic power in the form of oscillations. This produced acoustic power is directed through the resonator tube to the TAR stack where it gets utilized in producing a useful cooling effect. In the entire TADTAR, the TAE stack is the only work producing component whereas other components i.e., heat exchangers, resonator, and the TAR stack are the work consuming components. While in operation, acoustic work produced by the engine stack is used in overcoming resistance or impedance offered by these work consuming components. The TAE works as a reservoir of acoustic power for a TADTAR and higher the acoustic work production the more is the scope to convert this acoustic power into useful cooling.

2. Literature review

The TADTAR system contains no moving components and hence offers advantages such as mechanical simplicity and high reliability. This system can be built by using commonly available materials. It can be operated by using secondary sources of energy such as solar energy or industrial waste heat or any other low-grade energy source. This device uses environmentally friendly working gases, and this can even work on a mixture of gases.

Thermoacoustic technology also has a reasonable application base. One example is natural gas liquefaction [7].

Poese et al [8] showed thermoacoustic cooler as a potential device for ice cream sales. Swift [9] and Ovando et al [10] in their studies showed the possibility of generating electricity using thermoacoustic technology. Yu et al [11] devised an electricity generator by using an innovative concept of a traveling wave engine. In one of the most recent work, Abdoulla-Latiwish et al [12] came up with a micro-level electricity generator based on a traveling wave engine. This generator can deliver around 20 W of electricity when operated by waste heat from daily cooking activities. Besides these, thermoacoustic engines are used to drive pulse tube coolers [13, 14] to achieve cryogenic temperature and to separate a gas from a binary gas mixture [15].

Having recognized the advantages and usefulness of thermoacoustic technology, researchers across the globe have paid attention to this developing technology to devise sustainable cooling solutions. In one of the very first attempt, in 1989, Wheatley et al [16] designed a simple heat-driven TAR which had no moving parts at all. Though the attempt was appreciable, it was inefficient for a modest cooling temperature span. With increasing interest in TADTAR, researchers explored an alternative source of energy to drive TAE in the combination system. Amongst a very few standing wave configurations, Adeff et al [17] designed a 31.57 cm long solar-powered TADTAR. They focused the solar radiation using a Fresnel lens and directed the heat to the hot side of a TAE stack, eliminating the need for a hot heat exchanger. Their device produced 2.5 W of cooling power at a cold end temperature of 278 K, generating a total temperature difference of 18 K across the TAR stack.

Luo et al [18] extended the research in the field of traveling wave configuration by developing a TADTAR with two distinct traveling wave loops. The device upon operated at 57.7 Hz frequency and 3 MPa charging pressure, achieved system COP of 0.12 delivering 250 W of
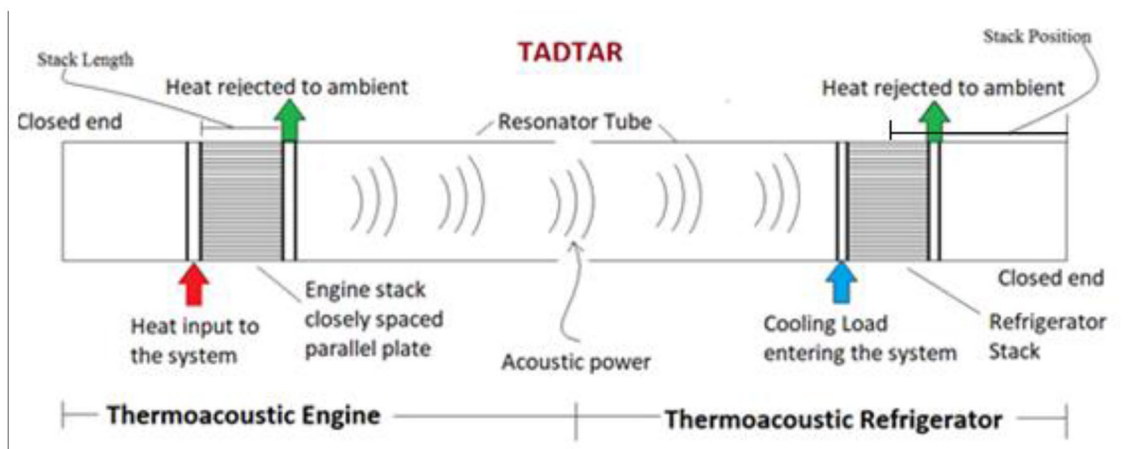
Figure 1. Schematic of a half-wavelength type, thermoacoustically driven thermoacoustic refrigerator.

cooling power at the temperature of 251 K. Kang *et al* [19] proposed a novel arrangement of a traveling wave cooler to be driven by a cascade TAE. It comprises a standing wave TAE, a traveling wave TAE and a traveling wave TAR in succession. With this configuration, at 75 Hz operating frequency and 2.5 MPa mean pressure, the cooler produced a 103 K temperature difference across the TAR stack. This temperature difference is among the highest recorded by a TADTAR device. Tasnim *et al* [20] experimented with the position of TAE stack and found the dependence of refrigerator performance in terms of cold end temperature. They used a cartridge heater as a source of heat supply and square cell Celcor ceramic stack in their experimental set-up. The length of the resonator tube of their device was 40 cm having stacks of 2.2 cm diameter and 2.5 cm length. They could obtain a cooling power of 0.11 W with 96 W heating powers and 10 K temperature difference across TAR stack. Hariharan *et al* [21] conducted an experimental study to check the effect of stack spacing on the temperature difference of TADTAR. They used twin standing wave thermoacoustic engines operating at 1 MPa and Mylar as stack material in their study. They observed better temperature difference with 0.4 mm spacing as compared to 0.8 mm spacing and reported a maximum temperature difference of 16 K across TAR stack.

Desai *et al* [22] presented a theoretical study wherein they solved equations of heat and work, using the linear theory of thermoacoustics and normalization, to calculate the efficiency of a TAE. They varied the hot end temperature of TAE from 400 K to 700 K and charging pressure from 1 MPa to 4 MPa. It is emphasized that the performance of a TAE depends upon the length and position of a stack besides operating temperature and charging pressure. This trend was found to be the same for every working fluid, namely Helium, Neon, Argon, and Carbon dioxide. It is also observed that the efficiency of a TAE is very sensitive to the length and position of the stack, and there is a definite length-position combination for a thermoacoustic device to achieve optimum performance for every working fluid. Further, they extended their work to TADTAR and used response surface methodology as an optimization tool [23]. During this work, their earlier finding of length and position combination is further strengthened by using a more convincing DeltaEC model. They reported a very sensitive dependence on the performance of a TADTAR on length and position.

During one of the most recent work, Alcock *et al* [24] carried out experiments on inline adjustable thermoacoustic engine driven thermoacoustic refrigerator. They studied different configurations of TAR stacks and stack positions with a stack diameter of 10.3 cm. They conducted a parametric study to show the effect on theoretical COP, sound pressure, the experimental temperature difference across TAR stack, and frequency of oscillations. They designed a system with resonator varying from 1.625 m to 2.125 m and reported a maximum temperature difference of 11 K across

TAR stack. While experimenting, they followed a methodology to vary TAR stack length and position by using different couplings in the existing experimental setup. However, by changing the stack position in this manner, the overall geometry, i.e., the length of a TADTAR system gets altered and hence response under the investigation is under the influence of multiple parameters. Following this methodology, the dependency analysis of the frequency of oscillations and sound pressure on the TAR stack position becomes imprecise. In the present work this misinterpretation is avoided by designing the system in such a way that upon varying the TAR stack position, the effect of a single parameter under investigations is derived. Saechan *et al* [25] built a traveling wave configured looped tube engine-cooler. The focus of this work was to demonstrate a sustainable cooling solution for rural communities in developing countries. The heat was supplied by a propane gas burner; the air was used as a working medium and PVC as a material of construction. They studied the location of the stack in traveling wave configuration to attain optimum cooling performance and achieved a lowest no-load temperature of 264 K suggesting the dependence of cooling performance on stack location.

In recent years, some researchers have numerically investigated the TADTAR. Khripach *et al* [26] presented a method for analyzing the exhaust gas cooler, which also found to help reduce the noise of an exhaust stream of an automobile. Their study focused on the porosity of a stack and suggested an enhanced performance with higher porosity of stack. Balonji *et al* [27] described a numerical model built within DeltaEC and conducted theoretical investigations on the adjustable resonator. The focus was to develop understandings of the performance of TADTAR in terms of the temperature difference across TAR stack, frequency of oscillations, acoustic power, and thermal efficiency of the device. From their DeltaEC model, they suggested a lower frequency of oscillations and lower sound pressure with an increase in resonator length.

With increasing interest, some researchers simultaneously touched upon the area of the working fluid. It is known in thermoacoustics that within the viscous penetration depth, acoustic power dissipation takes place which adversely affects the performance of a thermoacoustic system. The Prandtl number, a dimensionless number describing the ratio of kinematic viscosity to thermal conductivity, is a significant parameter for a thermoacoustic system. The Prandtl number for hard-sphere monatomic gases is 2/3. Mixtures of light and heavy monoatomic gases can fetch lower values of the Prandtl number. Tijani *et al* [28] presented experimental investigations to check the effect of Prandtl number, by using gas mixtures, on the performance of a TAR. Prandtl numbers ranging from 0.2 to 0.67 were obtained by using gas mixtures of Helium–Argon, Helium–Krypton, and Helium–Xenon. The measurements showed that the performance of the TAR enhances with decreasing the Prandtl number. An

improvement of 70% in COPR with a mixture of 70% Helium-30% Xenon as compared to that with 100% Helium was noted. Setiawan *et al* [29] numerically showed that using Helium based binary gas mixture; critical temperature difference of a TAE can be lowered. A lower critical temperature gradient is always advantageous for having an earlier onset of oscillations. They found that the lowest critical temperature varies with composition and operating pressure range while investigating with Helium, Nitrogen, Oxygen, Carbon dioxide, and mixtures.

From the reviewed literature, it is seen that researchers have worked in the field of TADTAR with both the configurations, standing wave type, and traveling wave type. However, it is also observed that the work done with TADTAR is in discrete sub-fields and there is no particular reference geometry available for a validation purpose. Additionally, much work is reported with traveling wave configuration as compared to that with a standing wave configuration. Length and position study of a TADTAR is available in theoretical form but experimental investigations for the same are found to be absent. Moreover, an experimental study of a TADTAR with different gases and gas mixture is also found to be unavailable. These shortcomings, observed in the literature and cited above are attempted in the present work. One of the prime objectives of this paper is to demonstrate the effect of stack position of a TAR, length of the resonator, and working fluid on the output of a TADTAR and to compare the temperature difference developed during present work to literature.

3. Experimental set-up

As mentioned in section 1, the engine of a TADTAR uses heat as input and produces acoustic power which is directed to the refrigerator to produce effective cooling. A thermoacoustic system mainly comprises of four components viz. a stack – often called as a heart of a thermoacoustic system, a resonator, and two heat exchangers. In individual TAR an additional component in a loudspeaker is used as an acoustic power source whereas an individual TAE can have a separate heating arrangement or can have heating arrangement integrated with hot heat exchanger. The present thermoacoustic system is a TADTAR wherein loudspeaker of a TAR is replaced by a TAE and hence this system comprises two stacks and four heat exchangers. Also, the TAE section of present TADTAR is kept unaltered and only the TAR section is altered by varying stack positions. A brief detail of these components is explained hereunder.

3.1 *The hot heat exchanger of TAE*

An internal electric coil heater is used as a heat input source to the TADTAR and working as a hot heat exchanger of a

TAE as shown in figure 2. It is joined to the SS304 housing which has a flanged connection with 8 holes for bolts. This housing is further connected to the resonator through a flanged connection. Fixing up of heater with housing has been one of the challenging tasks as this is the only part of a TADTAR which is subjected to high temperature and high pressure. Figure 3 shows the heater assembled to the SS housing. This housing has ID 58 mm with a 9 mm thickness. Wherever applicable, all the parts are designed to sustain internal pressure of 6 MPa.

3.2 *Stack*

It is the stack where the thermoacoustic phenomenon takes place. A steep temperature gradient is maintained across the TAE stack under the pressurized condition and due to heat exchange, acoustic oscillations are induced. However, in TAR, a temperature gradient gets established across the stack due to the heat transfer and heat transport process. The theory of thermoacoustic is well established and a quantitative engineering approach to the design of TAR is given by Tijani *et al* [6] and an analogous design approach for TAE has been provided by Desai *et al* [22]. The present TADTAR includes two stacks, one on the engine side and the other on the refrigerator side.

Stack in the present work is of parallel plate type, as shown in figure 4, which is nothing but closely spaced plate stacked together. The figure also defines plate spacing and plate thickness. This plate spacing is decided by the thermal penetration depth of a gas, equation (1) and generally, it is kept two to four times penetration depth [30]. If the gap is more, no heat transfer will take place and if the gap is less, then the viscous effect will adversely affect heat transfer.
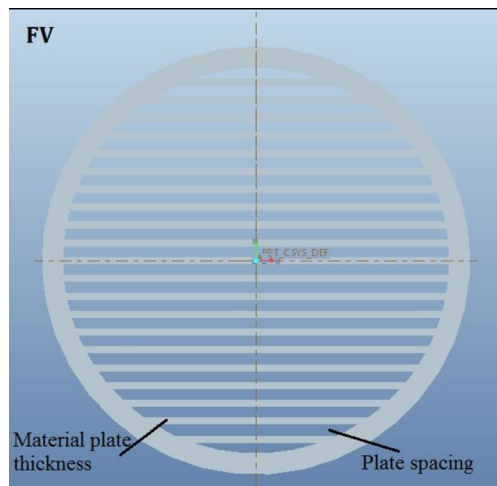
$$\delta_k = \sqrt{\frac{2k}{\rho \omega C_p}} \qquad (1)$$

Figure 2. Photograph of an internal electric coil heater of a TADTAR.
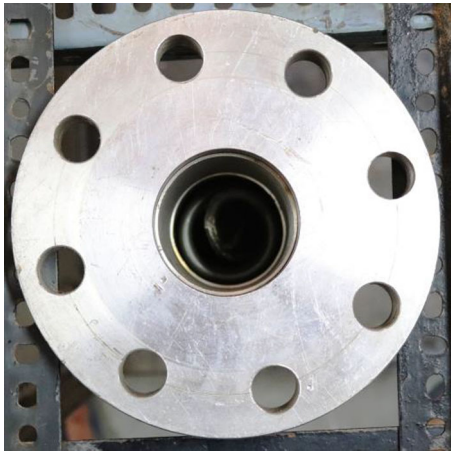
Figure 3. Photograph of heater-housing assembly.

Figure 4. A cross-sectional view of the stack model.

where, (k) is thermal conductivity, (ρ) is density, (C_p) is the isobaric specific heat of gas and (ω) is the angular frequency of oscillations. Similarly, the thermal penetration depth of material and consequently plate thickness can also be found using properties of stack material in equation (1). Work carried out by Swift [5] and Tijani *et al* [6] may further be referred to understand the heat transfer mechanism in detail.

Moreover, it is already a fact that acoustic power has a linear relation with mean pressure and frequency whereas it is seen from the equation (1) that thermal penetration depth is inversely proportional to mean pressure and frequency. Considering these two conditions, it is also understood that there has to be a compromise with stack performance while designing the stack because designing of stack largely depends on constructional feasibility. Contemplating the above-discussed points, plate thickness and plate spacing is

decided. Geometric details of these stacks are given in table 1.

Additionally, the stack material is expected to possess low axial thermal conductivity to impede heat conduction in the reverse direction in the case of the refrigerator, and simultaneously it should be able to hold parallel plate configuration along the length. In the present work, SS304 is used as a material of construction because the use of SS304 as stack material can easily sustain parallel plate configuration along the length of the stack. On the other hand, some in-house fabricated stack made of Mylar material would not guarantee standardization and there were chances of varying stack dimensions along the length of the stack. Besides this, to avail of some experimental flexibility, the same stack is also used in the engine section where other material (Mylar) cannot sustain due to high heat.
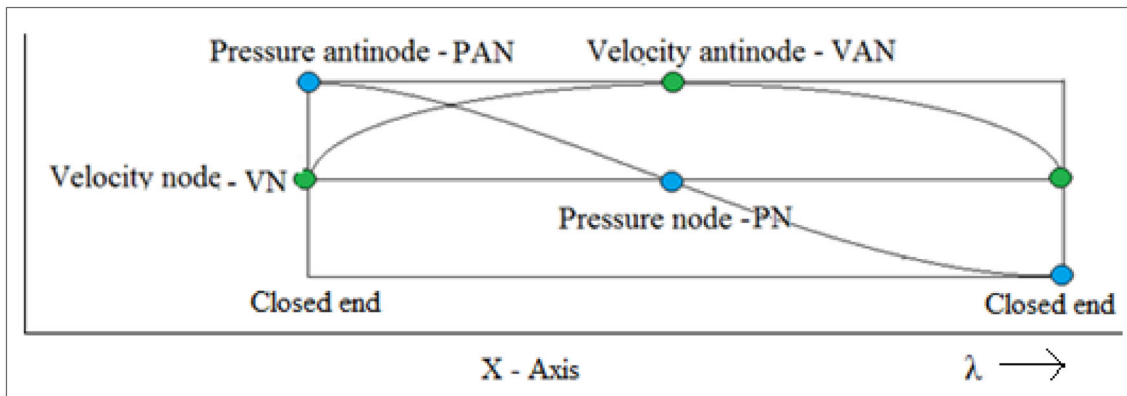
3.3 *Resonator*

The resonator is a very important component of a thermoacoustic device because the frequencies of oscillations, as well as pressure and velocity profiles, are significantly influenced by it. Configuration of a thermoacoustic system whether half-wave or quarter-wave is decided from the resonator. The present TADTAR demonstrates a half-wave type configuration by combining two quarter-wave type system.

In half-wavelength standing wave type TADTAR, there are pressure antinodes (PAN) at both the ends while the velocity antinode (VAN) is at the center as shown in figure 5. Since this is a standing wave type device, there exists a phase difference of 90° between pressure and velocity. Due to this, there is a pressure node (PN) at the center and velocity nodes (VN) at the closed end. Antinodes are the points where there is maximum deflection in absolute value to mean and nodes are the point where there is no deflection in absolute values to mean.

Resonator contains working fluid, transfers acoustic power, helps in sustaining acoustic oscillations and all the components get attached to the resonator. It should have enough strength to bear the high pressure of the gas. In the present work, the resonator is made from a 4.85 mm thick

Table 1. Geometric details of stacks.

Material of construction	Stainless steel SS 304
Plate thickness (mm)	0.14
Plate spacing (mm)	0.27
Porosity	66%
Diameter (mm)	60
Length of TAE stack (mm)	70
Length of TAR stack (mm)	50

Figure 5. Half-wavelength type thermoacoustic system with pressure and velocity nodes and antinodes.

SS304 pipe. To reduce acoustic power loss in a resonator, the diameter of the resonator pipe is reduced from 60 mm to 32.5 mm. This diameter reduction is carried out by using cone assemblies on either side of the resonator as shown in figures 6-8.

In the present work, the resonator is used as a geometric parameter and hence it is fabricated in two different lengths, denoted by R1 and R2, as shown in figure 6. These resonators have flanged joints and connected using gaskets in between. These gaskets serve a dual purpose of maintaining leak-proof joints and acting as thermal insulators against conduction heat loss in resonator.

3.4 *The ambient heat exchanger of TAE and TAR heat exchangers*

Heat exchangers are employed on both the ends of the stack and the main function of heat exchangers is to exchange heat with the surrounding. In TAE, the hot side heat exchanger consumes heat from a source and a cold side heat exchanger transfers the heat to surrounding in a quest to keep its temperature ambient. By doing so, a sharp temperature gradient across the TAE stack is retained which is the pre-requisite of TAE. In the current case, an annular type of copper heat exchanger has been used on the cold side of TAE where water flows through a circular annulus. This heat exchanger is also having a parallel plate type configuration with porosity same as that of the stack. In TAR, temperature gradient gets developed and that can be maintained by exchanging heat with the surrounding. Copper mesh has been cut in a circular shape to be used as heat exchangers for TAR which is placed adjacent to the TAR stack.
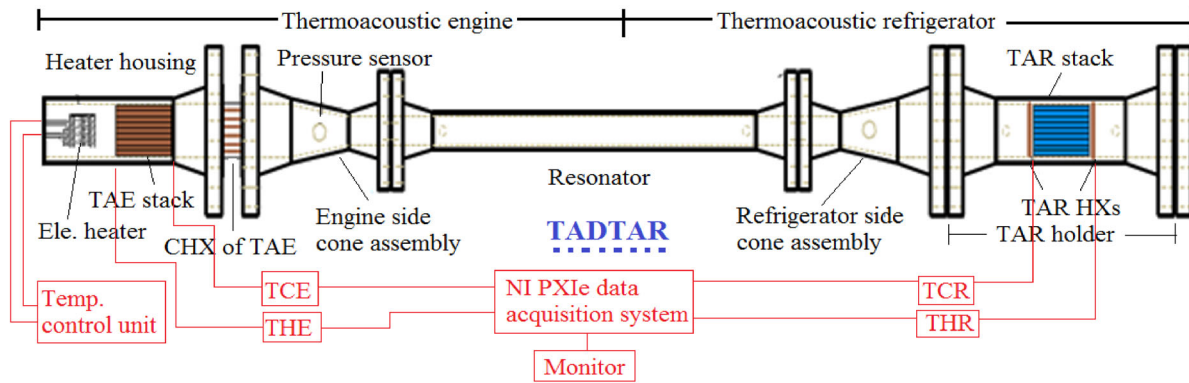
3.5 *Instrumentation and data acquisition system*

Figure 7 shows a schematic of a complete TADTAR system with instrumentation and data acquisition system and figure 8 shows the actual experimental set-up.

In the present study, heat input is given by the electric heater with the help of PID controlled temperature control unit. The pressure is measured, at the nearest possible location to the TAE side pressure antinode, as shown in figure 7, with the help of pressure transducer. This piezoresistive pressure transducer is further connected to the data acquisition system. The temperature is measured by k-type thermocouples calibrated, in-situ, in the span of 5-40 °C using a constant temperature bath. In total, the temperature is measured at four positions viz. hot side of TAE (THE), cold side of TAE (TCE), hot side of TAR (THR), and cold side of TAR (TCR) as shown in figure 7. These temperature sensors are also connected to the NI-PXIe data acquisition system. Acquired data are visualized through Labview software in the attached display monitor

Figure 6. Resonators.

Figure 7. Schematic of a TADTAR system including instrumentation and data acquisition system.
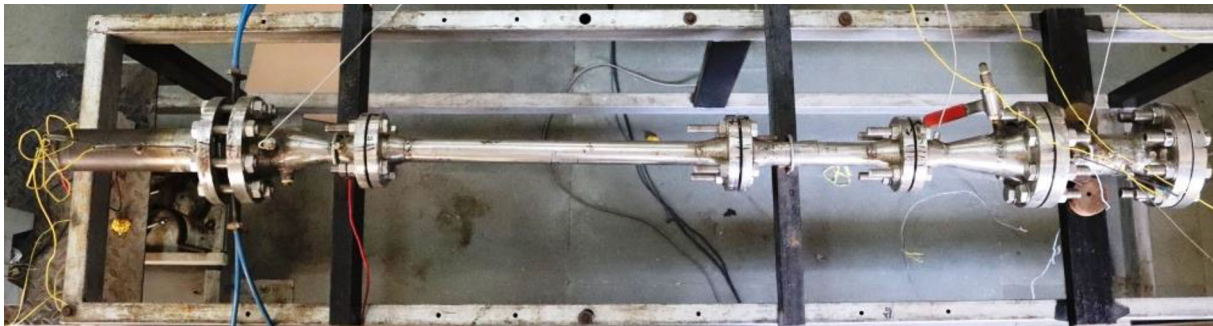
Figure 8. Photograph of the experimental set-up.

and this recorded data is further processed on a personal computer.

3.6 *Uncertainty analysis*

Based on the calibration, direct measurements associated with temperature are accurate within ±0.1 °C and the uncertainty associated with the derived quantities, pressure amplitude, and temperature difference may be considered as mentioned hereunder. However, frequency is directly observed through the Labview assisted data acquisition system. The maximum uncertainty in the temperature difference can be calculated as $u(\Delta T) = \sqrt{2 \times u(T)^2} = \sqrt{2 \times 0.1^2} = \pm0.141$ °C. Similarly, the pressure sensor has uncertainty $\pm0.2\%$ of full scale, that it 1000 psi, as per calibration report given by the supplier. The maximum uncertainty in the pressure amplitude can be calculated as $u(p_0) = \sqrt{2 \times u(p)^2} = \sqrt{2 \times 0.2^2} = \pm0.283\%$. Moreover, out of the total of 27 experiments, 7 random experiments are repeated to check reproducibility, and results are found

Table 2. Uncertainty values associated with measured quantities.

Sl. No.	Quantity measured	Uncertainty	Unit
1	Temperature	±0.1	°C
2	Temperature difference	±0.141	°C
3	Pressure	±0.2	%
4	Pressure amplitude	±0.283	%
5	Frequency of oscillations	–	–

to be acceptable. The results of the uncertainty calculations are shown in table 2.

4. Experimental parameters

In the present experimental work, two geometric parameters, resonator length and stack position of TAR, and one operating parameter in working gas is varied to carry out experimental parametric investigations. Details of variation are provided hereunder.

4.1 *Resonator variations*

The resonator is used as a geometric parameter for experiments and hence two resonators are fabricated, one a shorter and another longer as shown in figure 6. These two configurations amongst themselves give another variation of the resonator. Details of all three resonators are mentioned in table 3. The resonator is connected with the main system with the help of cone assembly on both sides as can be seen from figure 8. The length mentioned in table 3 is the effective length of a resonator i.e., inclusive of cone assemblies and connecting flanges.

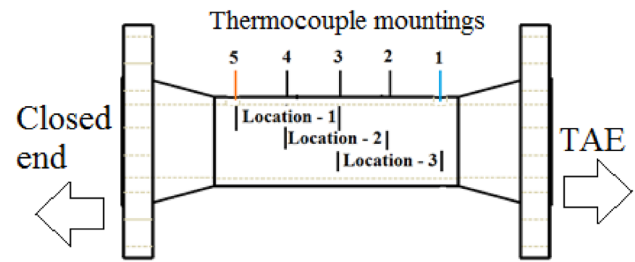### 4.2 *TAR stack position variations*

Dependence and sensitivity of the performance of a TAD-TAR on length and position are already discussed in an earlier section and due to that only the position of TAR stack has been considered as a parameter in the present work. As shown in figure 9, the refrigeration part of the current TADTAR system - termed as a TAR holder, is designed such that TAR stack with the heat exchangers of TAR can be accommodated within it.

Moreover, the TAR holder has feasibility that all three components together can be moved within it to have varying stack location and ultimately stack position variation, without changing the overall configuration of the experimental set-up. By doing so, the best location giving a better cooling performance, for a given system configuration, can be examined without altering the length of the set-up as against done by Alcock *et al* [24]. Thus a pure effect of stack position on other output parameters such as pressure amplitude and frequency of oscillations can be examined.

Provision is made to mount five thermocouples on TAR holder as shown in figure 9 which creates three different locations for TAR stack as a near ambient heat exchanger of TAR, at the center of TAR holder and near cold heat exchanger of TAR. Details of these location arrangements are mentioned in table 4.

4.3 *Working gas variations*

Another variation in the present work is the working medium. Three different gases namely Helium, Argon, and He50Ar50 – that is a gas mixture of 50% Helium and 50%

Table 3. Resonator configuration.

Resonator configuration	Designated as	The effective length of the resonator (m)
Only shorter	R2	0.770
Only longer	R1	1.100
Both together	R12	1.400

Figure 9. TAR stack location.

Argon are used as working fluid at 4 MPa charging pressure. Variations of working gas have been mentioned in table 5.

5. Experimental pre-requisites and methodology

Before starting of each experiment, stack and resonator are arranged as per predefined order to assemble TADTAR and simultaneously remounting of the TAR side thermocouples.

After the assembly of TADTAR, a leak test is conducted by charging Nitrogen gas at 4 MPa. The system is left untouched for 6 hours and is observed for any leakage by monitoring inside pressure through a data acquisition system that can show real-time data. When no change in pressure is observed during the above-said duration, the system is said to be leak-proof, and gas is released through a hand shut valve. The present system has too many joints and it requires repeated assembling and dismantling for this study, hence to save cost, initially leak test is conducted with Nitrogen.

The vacuum line is activated and all the unwarranted particles are flushed out before again carrying out the leak test with actual working gas for a particular experimental run. Again aforesaid leak test procedure is followed until the system is found to be leak-proof. Thermocouples are then reconnected with the NI-PXIe data acquisition system.

Once the system gets stabilized, the heater is turned on through the temperature control unit and then hot end temperature is increased till the onset of oscillations is observed. Upon observing the onset, TAR temperature readings are tracked until it gets saturated and at the same time, the frequency of oscillations is also recorded from the data acquisition display. Once the system reaches a saturation state, the heat supply is cut off in the decremented manner before turning off the heater. As soon as the system gets normalize, it is dismantled for the next experimental run.

6. Results and discussion

Experiments are carried out on a TADTAR with the gas mixture as a working fluid to analyze the influence of an operating parameter. The effect of two geometric

Table 4. Details of the stack position.

TAR stack location	Configured as	Designated as	Stack position (mm)
Near ambient heat exchanger of TAR	Location 1	L1	95
At the center of TAR holder	Location 2	L2	135
Near cold heat exchanger of TAR	Location 3	L3	175

Table 5. Details of working gas variations.

Gas	Configured as	% of Helium	Prandtl Number	Acoustic velocity (m/s)
Helium	He	100	0.6793	1019.2
Helium - Argon Mixture	HeAr	50	0.4178	434.94
Argon	Ar	0	0.6626	322.58

parameters, TAR stack position and resonator length, are also assessed on the performance of TADTAR. The stack position of a TAR is varied in such a way that the overall geometry of a TADTAR system remains unaltered. All these parameters are varied with three distinct choices as discussed in the previous subsection. The performance of a TADTAR is evaluated by measuring temperature difference across TAR stack, frequency of oscillations, and pressure amplitude in the TADTAR system. During this experimental study, the maximum pressure amplitude of 82.96 kPa and a maximum temperature difference of 16.3 K across the TAR stack have been recorded.

For all the following plots, legend R followed by a number stands for resonator configuration as mentioned in table 3.

6.1 *Effect on the frequency of oscillations*

Figure 10 shows the effects of resonator length, TAR stack position, and working gas on the frequency of oscillations of TADTAR. It is noticeable that for a TADTAR, the frequency of oscillation varies marginally and grossly independent of the placement of refrigeration load. This relation remains valid for all positions of TAR stack for all configurations of resonators and all combinations of working gas. This experimental finding is more generalized for a TADTAR because in the present work while changing the position of TAR stack, overall geometry was kept unaltered as against done previously [24].

It is well versed that for a half-wave thermoacoustic system, frequency and length of the resonator are related as expressed in equation (2).

$$L = \frac{\lambda}{2} \qquad (2)$$
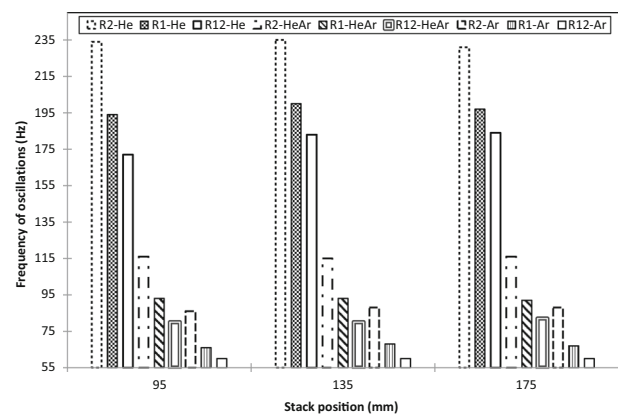
Figure 10. Effect of resonator length, TAR stack location, and working gas on the frequency of oscillations.

where, (L) is the length of resonator and (λ) is the wavelength. This equation can be rearranged as expressed by equation (3).

$$f = \frac{a}{2L} \qquad (3)$$

where, (f) is the frequency of oscillations and (a) is the acoustic velocity of the gas.

As it is seen from equation (3) that frequency and length of the resonator are inversely proportional to each other and hence the frequency of oscillations decreases with increase in the length of the resonator as can be seen from figure 10 for all three gases and all three position of the TAR stack.

Moreover, it can also be noted from equation (3) that the frequency of oscillation varies linearly with the acoustic velocity of the gas. Helium, having the highest acoustic velocity amongst the gases being discussed, shows the

maximum frequency of oscillations followed by He-Ar mixture and Argon respectively for all the variations of resonator and TAR stack position. The frequency of oscillations increased from an average 60 Hz to 88 Hz with a decrease in resonator length from 1.4 m to 0.77 for Argon gas. Similarly, the frequency of oscillations for He-Ar mixture and Helium gas increased from an average 80 Hz to 116 Hz and 180 Hz to 233 Hz respectively with a decrease in resonator length from 1.4 m to 0.77 m. Overall, the frequency of oscillations varies in the range of average 60 Hz for the longest resonator and Argon gas to 233 Hz for the shortest resonator and Helium as working gas.

As mentioned previously, frequency is directly captured through LabVIEW software and an example of the same is shown in figure 11 for Argon gas with resonator R12. The highest average frequency of 233 Hz is recorded with the shortest resonator - R2 and Helium gas. Whereas the lowest average frequency of 60 Hz is recorded with the longest resonator - R12, and Argon as a working gas.

6.2 *Effect on pressure amplitude*

As one of the ways of estimating the intensity of thermoacoustic oscillations, pressure amplitude is treated as an important parameter. In a TADTAR, as discussed in section 1, pressure amplitude shows the reserve capacity of a TAE in terms of acoustic power. Higher pressure amplitude shows a better capacity of the TAE section in overcoming impedance offered by acoustic work consuming parts including TAR stack. Contrary, higher pressure amplitude shows that TAE is producing more acoustic power than being consumed within TADTAR. So it is capable of producing more cooling provided the precise placement of TAR stack for efficient conversion of acoustic power into cooling effect. The effects of resonator length, TAR stack position, and working gas on pressure amplitude is shown in figure 12. The results show that higher pressure amplitudes are recorded with an increase in resonator length irrespective of working gas.
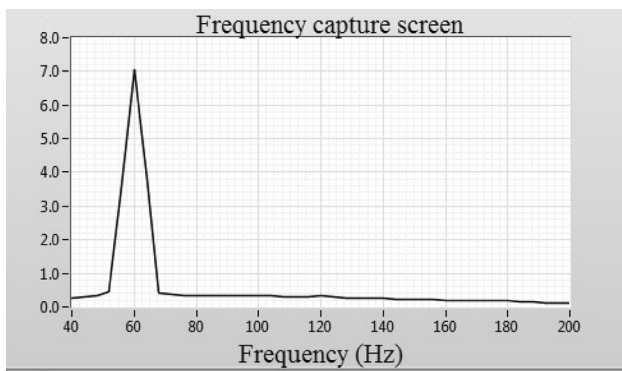
This is because, for a fixed configuration of TADTAR, with an increase in resonator length, TAE stack automatically gets shifted towards pressure antinode and hence higher pressure amplitudes are observed. It is also seen that the pressure amplitude of a TADTAR system decreases with an increase in the TAR stack position.

In terms of working gas, higher pressure amplitude is recorded with Argon gas followed by He-Ar mixture and Helium respectively regardless of the resonator length and TAR stack position. This is because, with Argon gas, the higher impulse can be realized due to the higher value of the product of density and acoustic velocity. Argon possesses the highest value of (ρa) followed by He-Ar mixture and Helium respectively and the effect of this factor can be visualized from figure 12 as well. This basic understanding regarding pressure amplitude remains unchanged even after the inclusion of the refrigeration load. The maximum pressure amplitude is recorded with the TAR stack being nearest to the closed end, with a combination of the longest resonator R12 and Argon as a working fluid. The minimum is recorded with TAR stack being farthest from the closed end with the shortest resonator R2 and Helium as a working gas.
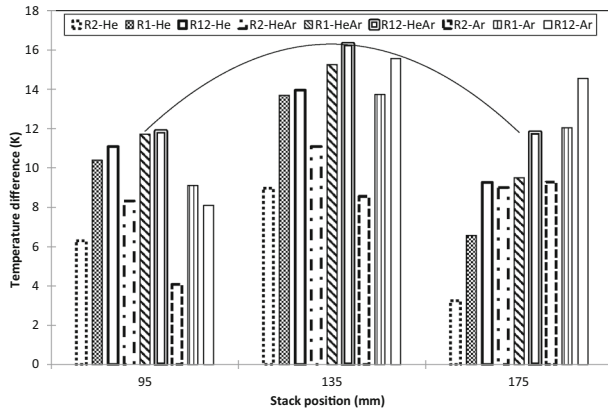
6.3 *Effect on the temperature difference across TAR stack*

Figure 13 shows the effect of resonator length, TAR stack position, and working gas on temperature difference across the TAR stack. Results show that with an increase in resonator length, for a fixed configuration, temperature difference increases. This is because increased resonator length increases pressure amplitude as seen in the previous section and this higher pressure amplitude help in achieving better temperature difference.

Moreover, it is interesting to mark that all the configurations show better cooling performance in terms of the temperature difference across TAR stack at location L2,

Figure 11. Frequency captured for Argon gas and resonator R12.
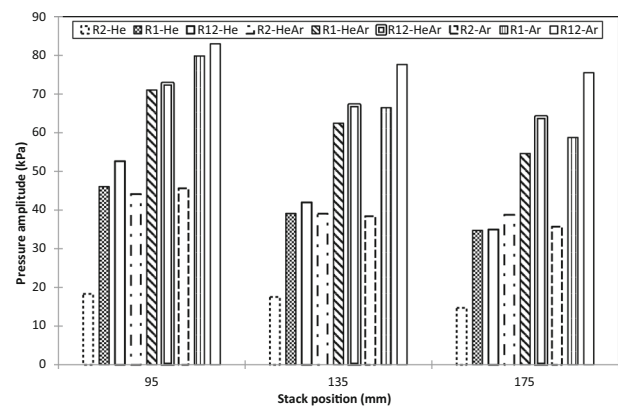
Figure 12. Effect of resonator length, TAR stack location, and working gas on pressure amplitude.

Figure 13. Effect of resonator length, TAR stack location, and working gas on temperature difference across TAR stack.

which is a central location, a stack position of 135 mm. This finding is backed by the theoretical results [22, 23] that there exists a unique length-position combination for a stack of a thermoacoustic device where an optimum performance can be attained. From figure 13 it can be concluded that the position of TAR stack plays a vital role in designing TADTAR.

While studying the effect of working gas on temperature difference across TAR stack, for all the variations it is found that He-Ar mixture fetches the maximum temperature difference due to its lowest Prandtl number as can be seen from table 5. The magnitude of temperature difference achieved by the He-Ar mixture is succeeded by Argon gas and Helium gas respectively. This finding is backed by a study carried out by Tijani *et al* [6] wherein it has been demonstrated that by lowering the Prandtl number, viscous effects can be lowered which eventually helps in achieving better thermoacoustic performance. In the present TADTAR, the maximum temperature difference of 16.3 K is recorded with the longest resonator R12 and He-Ar gas mixture as a working fluid. The advantageous stack position found from these experiments can be implemented for generating enhanced cooling using TADTAR.

7. Conclusions

In this experimental study, parametric variations are carried out to observe the frequency of oscillations, pressure amplitude, and temperature difference across the TAR stack. Within this section, concise results achieved in this study are reported.

- In this paper, due to a distinct experimental methodology, it is concluded that the frequency of oscillations is independent of the placement of refrigeration load as against mentioned in literature [24]. The frequency of oscillations of a TADTAR system depends only on resonator length and working gas.

- In a thermoacoustic system, even after the inclusion of refrigeration load i.e., TADTAR, pressure amplitude improves with an increase in resonator length and using heavier gas as a working medium.
- Comprehensively, it is experimentally validated that, similar to a thermoacoustic engine [18], there exists a unique length-position combination for a stack where a TADTAR attains optimum performance.
- From the present experiments, it is inferred that half-wavelength standing wave type TADTAR exhibits a higher temperature difference with a longer resonator configuration and He-Ar mixture as a working gas. The maximum temperature difference of 16.3 K is recorded during the present work.

Nomenclature

k	Thermal conductivity (W/m-K)
C_p	Specific heat at constant pressure (J/kg-K)
L	Length of resonator (m)
f	Frequency of oscillations (Hz)
a	Acoustic velocity of the gas (m/s)

Greek letters

δ	Penetration depth (m)
ρ	Density (kg/m^3)
ω	Angular frequency of oscillations (rad/s)
λ	Wavelength (m)

Sub-scripts

k	Thermal

Abbreviation

TADTAR	Thermoacoustic engine driven thermoacoustic refrigerator
TAE	Thermoacoustic engine
TAR	Thermoacoustic refrigerator
PAN	Pressure antinode
PN	Pressure node
VAN	Velocity antinode
VN	Velocity node

References

[1] Rott N 1969 Damped and thermally driven acoustic oscillations in wide and narrow tubes. *J. Appl. Math. Phys.* 20: 230–243

[2] Rott N 1975 Thermally driven acoustic oscillations, part III: Second-order heat flux. *J. Appl. Math. Phys.* 26: 43–49

[3] Rott N 1980 Thermoacoustics. *Adv. Appl. Mech.* 20: 135–175

[4] Rayleigh J W S 1886 *The theory of sound*. 2nd edition Vol. 2 Sec. 322. (Dover, New York, 1945)

[5] Swift G W 1988 Thermoacoustic engines. *J. Acoust. Soc. Am.* 84: 1145–1180

[6] Tijani M E H, Zeegers J C H and De Waele A T A M 2002 Design of thermoacoustic refrigerators. *Cryogenics* 42: 49–57

[7] Wollan J J, Swift G W, Backhaus S and Gardner D L 2002 Development of a thermoacoustic natural gas liquefier. *AIChE New Orleans Meeting*. 1–8

[8] Poese M E, Smith R W M, Garrett S L, Van Gerwen R and Gosselin P 2004 Thermoacoustic refrigeration for ice cream sales. *Web*

[9] Swift G W 1988 A liquid-metal magnetohydrodynamic acoustic transducer. *J. Acoust. Soc. Am.,* 83: 350–361

[10] Ovando G, Huelsz G, Ramos E and Cuevas S 2005 Effect of a magnetic field on the linear stability of a thermoacoustic oscillation. *J. Non-Equil. Thermodyn.* 30: 1–27

[11] Yu Z, Jaworski A J and Backhaus S 2012 Traveling-wave thermoacoustic electricity generator using an ultra-compliant alternator for utilization of low-grade thermal energy. *Appl. Energy* 99: 135–145

[12] Abdoulla-Latiwish K O A, Mao X and Jaworski A J 2017 Thermoacoustic micro-electricity generator for rural dwellings in developing countries driven by waste heat from cooking activities. *Energy* 134: 1107-1120

[13] Jin T, Chen G B and Shen Y 2001 A thermoacoustically driven pulse tube refrigerator capable of working below 120 K. *Cryogenics* 41: 595–601

[14] Tang K, Chen G, Jin T, Kong B, Bao R, Qui L and Gan Z 2004 92 K thermoacoustically driven pulse tube refrigerator. *Chinese Sci. Bull.* 49: 1541–1542

[15] Geller D A, Spoor P S and Swift G W 2001 Separation of gas mixtures by thermoacoustic waves. *Web*

[16] Wheatley J C, Swift G W, Migliori A and Hofler T J 1989 Heat driven acoustic cooling engine having no moving parts. *US Patent* No. 4858441

[17] Adeff J A and Hofler T J 2000 Design and construction of a solar-powered, thermoacoustically driven thermoacoustic refrigerator. *J. Acoust. Soc. Am.,* 107: 37–42

[18] Luo E, Dai W, Zhang Y and Ling H 2006 Thermoacoustically driven refrigerator with double thermoacoustic Stirling cycles. *Appl. Phys. Lett.* 88: 074102

[19] Kang H, Jiang F, Zheng H and Jaworski A J 2013 Thermoacoustic traveling wave cooler driven by a cascade thermoacoustic engine. *Appl. Therm. Eng.* 59: 223–231

[20] Tasnim S H and Fraser R A 2010 Thermal field measurements of a thermoacoustically driven thermoacoustic refrigerator. *J. Therm. Sci. Eng. Appl.* 2: 021010

[21] Hariharan N M, Sivashanmugam P and Kashturirengan S 2013 Experimental investigation of a thermoacoustic refrigerator driven by a standing wave twin thermoacoustic prime mover. *Int. J. Ref.* 36: 2420–2425

[22] Desai A B, Desai K P, Naik H B and Atrey M D 2016 Design and analysis of standing wave quarter wavelength thermoacoustic engine. *Indian J. Cryog.* 41: 69–74

[23] Desai A B, Desai K P, Naik H B and Atrey M D 2017 Optimization of thermoacoustic engine driven thermoacoustic refrigerator using response surface methodology. *IOP Conf. Ser. Mater. Sci. Eng.* 171: 012132

[24] Alcock A C, Tartibu L K and Jen T C 2018 Experimental investigation of an adjustable thermoacoustically-driven thermoacoustic refrigerator. *Int. J. Ref.* 94: 71–86

[25] Saechan P and Jaworski A J 2018 Thermoacoustic cooler to meet medical storage needs of rural communities in developing countries. *Therm. Sci. Eng. Prog.* 7: 164–175

[26] Khripach N A, Lezhnev L Y, Ivanov D A, Papkin B A and Korotkov V S 2018 Computational analysis of the exhaust gas cooler of an automobile engine. *Int. J. Pure Appl. Math.* 119: 2627–2631

[27] Balonji S, Alcock A C, Tartibu L K and Jen T C 2019 Performance alteration of standing-wave thermoacoustically-driven engine through resonator length adjustment. *Procedia Manuf.* 35: 1350–1355

[28] Tijani M E H, Zeegers J C H and De Waele A T A M 2002 Prandtl number and thermoacoustic refrigerators. *J. Acoust. Soc. Am.* 112: 134–143

[29] Setiawan I, Nohtomi N and Katsuta M 2015 Critical temperature differences of a standing wave thermoacoustic prime mover with various helium-based binary mixture working gases. *J. Phys. Conf. Ser.* 622: 012010

[30] Swift G W 1995 Thermoacoustic engines and refrigerators. *Phys. Today* 48: 22–28